JOURNAL OF SPACECRAFT AND ROCKETS
Vol. 39, No. 3, May–June 2002

Plasma Response to Arcing in Ionospheric Plasma Environment: Laboratory Experiment

Mengu Cho,* Raju Ramasamy,† and Masayuki Hikita‡
Kyushu Institute of Technology, Kitakyushu 804, Japan
and
Koji Tanaka§ and Susumu Sasaki¶
Institute of Space and Astronautical Sciences, Kanagawa 229, Japan

Laboratory experiments are carried out to study the response of plasma to a sudden potential change induced by arcing on a solar array in low-Earth-orbit plasma environment. A solar array is biased negatively in a plasma chamber with insulator simulating coverglass or thermal paint located remotely from the arc point. When an arc occurs, electrons are ejected from the arc point to the surrounding plasma, producing a negative sheath. Shortly after the arc onset, the influx of positive charge into the circuit causes a jump of the potential, and the positive sheath is formed near the insulator surface. If the positive sheath meets the negative sheath near the arc point while the conductivity of the arc plasma is still high, a current path is formed between the arc point and the insulator surface. The current path supplies the positive charge on the insulator surface to the arc current and feeds energy to arc plasma. Experimental results show that there is a safety distance beyond which arc plasmas cannot form the current path.

Nomenclature

B	=	magnetic field, G
C	=	capacitance, F
C_s	=	capacitance of insulator surface to the electrode, F
d	=	distance between array and capacitance, cm
I_n	=	neutralization current, A
I_p	=	peak of discharge current, A
m	=	particle mass, kg
n	=	number density, m^{-3}
Q_d	=	charge flown in one arc, C
Q_s	=	charge stored on insulator surface, C
R	=	resistance, Ω
T_e	=	electron temperature, eV
T_p	=	peak time of discharge current, s
T_{pr}	=	peak time of probe signal, s
t	=	time, s
V	=	potential, V
V_{array}	=	solar array output voltage, V
V_b	=	bias voltage, V
V_{pr}	=	probe signal, V
y	=	horizontal position, cm
z	=	axial position, cm
ΔV	=	change of spacecraft potential due to arc onset, V

Subscripts

e	=	electron
i	=	ion
n	=	neutral
ϕ_e	=	electrode potential, V
ϕ_s	=	insulator surface potential, V
ϕ_1	=	potential of the positive end of solar array, V
ϕ_2	=	potential of the negative end of solar array, V

Presented as Paper 2001-0955 at the AIAA 39th Aerospace Sciences Meeting, Reno, NV, 8–11 January 2001; received 22 March 2001; revision received 24 August 2001; accepted for publication 30 August 2001.

*Associate Professor, Department of Electrical Engineering, Tobata-ku; cho@ele.kyutech.ac.jp. Member AIAA.
†Postdoctoral Fellow, Satellite Venture Business Laboratory, Tobata-ku.
‡Professor, Department of Electrical Engineering, Tobata-ku.
§Research Associate, Space Energy Division, Sagamihara.
¶Professor, Space Energy Division, Sagamihara.

I. Introduction

TO promote industrial use of low Earth orbit (LEO), such as manufacturing, sightseeing, or power generation, the power of a large LEO platform that follows the International Space Station (ISS) may soon reach the level of megawatts. In principle, the transmission voltage scales to the square root of the power to be delivered to minimize the energy loss during power transmission and the cable mass. ISS with 100 kW is operated at 120 V. An experimental solar power satellite with 10 MW needs to be operated at least 1000 V (Ref. 1). Therefore, a space platform with 1-MW power must be operated at approximately 400 V. To realize 400-V operation in LEO, arcing caused by interaction between the spacecraft and the surrounding LEO plasma must be overcome.

When a spacecraft has a high voltage within its body and the high voltage surface is exposed, most of the high voltage becomes negative with respect to the electric potential of the surrounding plasma. Figure 1 shows a circuit layout of typical spacecraft. The spacecraft structural body that is made of conductor material serves as the grounding point of the circuit and is usually connected to the negative end of the array. Then, the spacecraft structural body has a high negative potential. The spacecraft body attracts positive ions from the surrounding plasma, and the ions impact the body surface and solar array. Many parts of spacecraft surfaces are made of electrical insulators, such as solar array coverglass or thermal coating materials, which are often also electrical insulator materials. Therefore, when ions impact spacecraft dielectric surfaces, the surfaces are positively charged. The positive charging continues until the surface potential reaches a value where the ion current to the surface is equal to the electron current, which is typically comparable to electron temperature κT_e and negligible compared to the body potential V. Therefore, the electrical insulator acts as a capacitance that stores the positive charge on the surface facing the plasma.

It is known that arcing can occur once there is an opening in the insulator where the underlying conductor with a negative potential of −100 V or larger, typically, is exposed to space.[2] The arcing is triggered by charging of insulator material via plasma and field intensification at the conductor surface, especially at the junction with the insulator, which is called a triple junction, because three

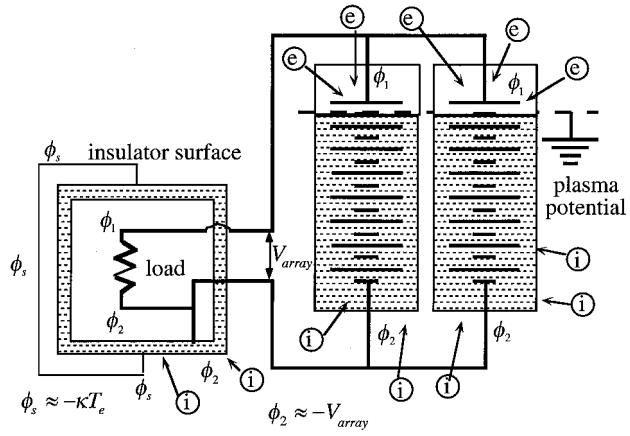

Fig. 1 Schematic of electrical circuit of spacecraft and potential with respect to the LEO plasma.

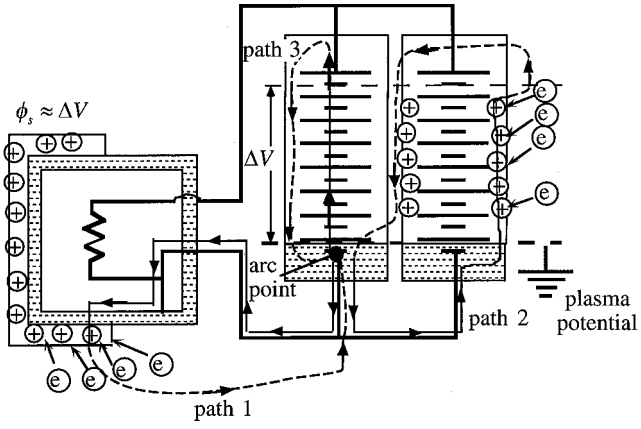

Fig. 2 Schematic of current paths to the arc point.

materials with different electrical conductivity (conductor, insulator, and vacuum), meet there. There are many ways for a triple junction to be formed. One example is an interconnector between solar cells, where the triple junction is formed with the interconnector exposed to space, the adhesive to attach coverglass, and the vacuum. Another example is a hole in the thermal paint exposing the underlying conductive surface produced by impact of a small particle on the surface. Arcing raises concerns with electromagnetic interference, surface deterioration, or even destruction of spacecraft circuits, which is demonstrated in Refs. 3 and 4. How much the arcing affects the spacecraft system depends on how much current and energy the arcing current carries into the spacecraft circuit. Previous experiments[5–8] indicate that, once an arc occurs on spacecraft insulator surface, the arc induces a significant current on the other parts of the insulator surface.

The purpose of this paper is to study via laboratory experiments how the arc current grows by receiving charge from the nearby insulators. In the accompanying paper,[9] we carry out a basic study on the growing mechanism via a laboratory experiment and computer simulation. Once an arc occurs at one point on a spacecraft surface, either solar array or body surface, the arc spot collects a large amount of positive charge in a short time, driving the spacecraft potential up. At the same time, electrons are ejected from the arc spot. The insulating surface becomes positive comparable to the array output voltage at maximum, exposing its positive charge on the surface to the electrons. Then, the surface charge is rapidly neutralized by the electrons, which results in a large negative current flowing through the spacecraft body circuit. This phenomenon is the capacitive coupling of the arc plasma with the spacecraft circuit. The current path is schematically shown in Fig. 2 as paths 1 and 2. Path 1 is the current path between the arc point and the insulator surface on the body, and the path 2 is the current path between the arc point and the solar array coverglass. The solid lines in Fig. 2 indicate the currents inside the spacecraft circuit, and the broken lines indicate the current through the plasma. This current path is essentially *RC* discharge, where *R* is given by the resistance of plasma and circuit and *C* is coverglass capacitance. This model of *RC* discharge feeding the energy to the arc plasma has been illustrated in Refs. 5 and 10.

This study is important in the sense that we need to know how much energy an arc can have. It is also important to know the condition by which an arc becomes more severe. Current paths 1 and 2 in Fig. 2 feed the energy to the arc plasma through the *RC* discharge. As the arc plasma grows and extends over the positive end of the array string, the plasma can short circuit the positive and negative ends of the array, shown as current path 3 in Fig. 2. This path 3 can be attached to the positive end of the same strings, as shown in Fig. 2, or of a different string and depends on the cell layout on the array surface. A typical solar array string can generate a current of several amperes at the solar intensity in LEO. If the arc plasma has a sufficient conductivity to maintain itself with that amount of current, the arc current keeps flowing, leading to destruction of the solar array circuit, a so-called sustained arc.[3,4] Initial growth of the arc plasma, therefore, is very important. The degree of growth determines whether an arc causes a fatal effect to the spacecraft circuit. Even if arcs end as single pulses, accumulative effects, such as surface deterioration like discoloration, peeling off, damage, and others, are determined by how large each single pulse is. In the present paper, we investigate both how far the surface charge of the unarced surface is neutralized by this mechanism and how the current path is connected into the spacecraft circuit using a model system in the laboratory experiment.

Recently, Cho et al.[11] found that a current path between the arc point and remotely located insulator is formed by arc plasma. They biased the combination of a solar array and an electrode wrapped by insulator film to a negative potential as high as −700 V in a large vacuum chamber of 2.5-m diam, where the LEO plasma condition was simulated. They tested two cases of the distance between the solar array and the electrode, 40 and 80 cm. The arc plasma could connect the arc point on a solar array and the insulator on top of the biased electrode even for the distance of 80 cm. The arc plasma, however, often failed to connect for the 80-cm case compared to the 40-cm case. Also, the time for the arc plasma to connect the two surfaces was longer for 80 cm than for 40 cm. A langmuir probe was used to measure the plasma condition at various points inside the chamber, and it was found that the space potential near the solar array became negative and that the potential near the insulator became positive, once an arc occurred at the solar array.

Based on these results, a model of the discharge path formation was proposed, which is schematically shown in Fig. 3. Once an arc occurs, electrons are ejected from the array to the surrounding plasma producing an electron-rich negative sheath. At the same time, injection of positive charge into the circuit causes a jump in the array potential and the electrode potential under the insulator toward zero from the highly negative value. Before the arc, the insulator surface potential is nearly zero, comparable to the electron temperature, typically 1 eV, to have the zero current condition at a steady state.

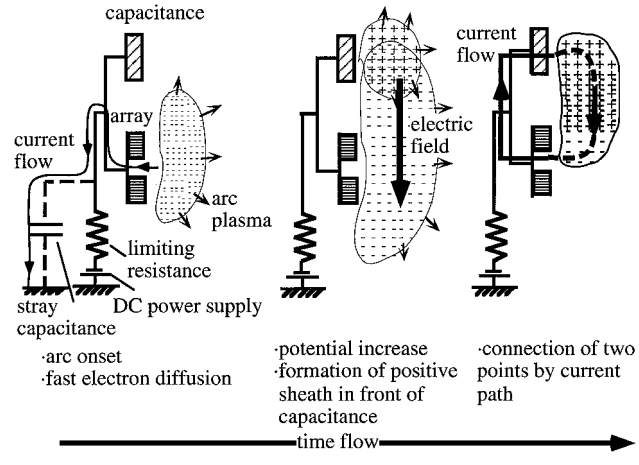

Fig. 3 Model of current path formation between arc point and unarced insulator surface.

Therefore, across the insulator, there is a potential drop nearly equal to the bias voltage, which is of the order of magnitude of 100 V. The jump of the electrode potential, which is several microseconds or less, also causes the jump of insulator surface potential from the near zero value to a positive value of the order of magnitude of 100 V. Then a positive sheath is formed near the insulator surface where the electric potential is positive. There is an electric field between the array and the insulator, and if the conductivity is high enough, the current path is formed.

In this study, we carry out new experiments and computer simulations to further validate the model of current path formation. The experimental setup is basically similar to the previous work,[11] but this time we have installed more test samples inside the chamber so that we can study how far the arc plasma can influence the remotely located insulator. Finding the safety distance of arc plasmas provide very important data to the design of high-voltage space systems. In the accompanying paper,[9] to investigate how the surrounding plasma responds to the sudden change of the insulator surface potential caused by arcing, we give an artificial jump of the insulator surface potential and carry out a controlled experiment. We also carry out computer simulation to visualize the phenomena occurring in the experiment. In the second section of this paper, we describe the laboratory experiment, which simulates solar arrays and remotely located capacitance under the LEO space plasma conditions. In the third section, we show the experimental results. Finally, we conclude the paper with suggestions for future experimental work.

II. Experiment

The vacuum chamber we used in the experiments was 4.0 m long with 2.5-m diam and was located at the Institute of Space and Astronautical Sciences. The axial length is 5.5 m if we include the semispherical noses at the both ends. The chamber had a diffusive argon plasma source located at one end, which generated plasma conditions of $n_e \sim 5 \times 10^{11}$ m^{-3} and $\kappa T_e = 2.4$ eV. The chamber pressure was $2 \sim 3 \times 10^{-4}$ torr while the plasma source was operating. To make the analysis easier, the Earth's magnetic field was canceled by external coils most of the time. Unless stated otherwise, the magnetic field B inside the chamber was kept less than 0.09 G.

We placed two small solar arrays and three capacitances inside the chamber, as shown in Fig. 4. The coordinate of each biased sample is given in centimeters. The cylindrical chamber is placed horizontally. Figure 4 shows the setup inside the chamber from the viewpoint as if we look down from the top. The arrays and capacitances were mounted on acrylic poles at the same height. One array was located at the chamber axis, which we call array 1. Another array was placed 70 cm left of array 1, which we call array 2. Capacitance 2 was placed 40 cm right of array 1. Capacitance 1 was placed 30 cm right of capacitance 2. Arrays 1 and 2 and capacitances 1 and 2 face the plasma source. Capacitance 3 was placed at the axis of the chamber facing array 1, 270 cm from array 1. To specify the probe position, we employed a coordinate system whose origin was at the surface of array 1, as shown in Fig. 4. The axial direction toward the plasma source is the z axis. The horizontal direction toward capacitance 1 is the y axis. In the present paper, the x axis is the vertical direction, positive x in the upward direction.

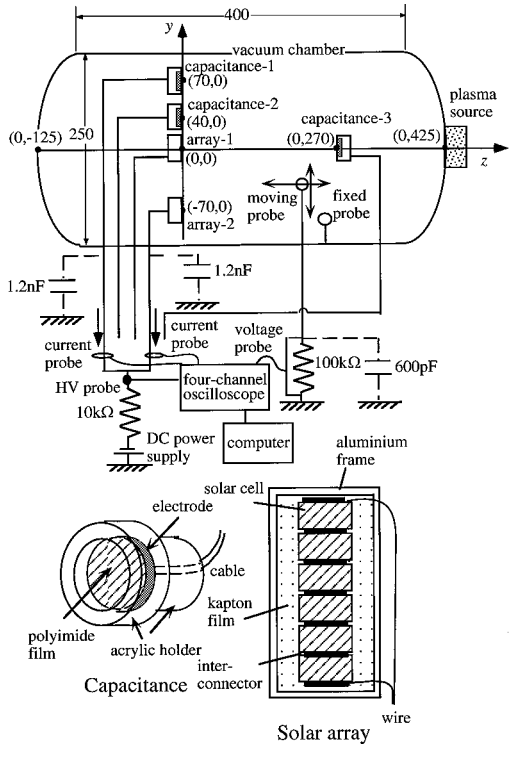

Fig. 4 Setup of arc experiment.

The capacitances simulated coverglass of remotely located cells from the arced interconnector. To increase the capacitance per unit area, thin polyimide film (7.5 μm thick, dielectric constant 3.5) was used instead of real coverglass ($\sim$100 μm, typically). The film was placed on top of a stainless-steel electrode, which was completely insulated by the film and acrylic holder. Capacitances 1 and 2 had 21 nF, and capacitance 3 had 5.2 nF because its radius was one-half of capacitances 1 and 2. Each solar array consisted of six Si cells connected in series with a separation distance of 0.8 mm. The size of each cell was 2×4 cm. The cells were glued on Kapton® film, and the film was fixed on an aluminum frame. The wires of the arrays were shortened and connected to a dc power supply to be biased to up to -800 V.

One array, either array 1 or array 2 and either capacitance 1 or 2 or 3 were biased at the same time by a dc power supply. The distance between the array and the capacitance from 40 to 270 cm was varied by changing the combination of bias. The current from each biased sample was measured by a current probe. The arrows at the current probe in Fig. 4 indicate the definition of the direction of the positive current. The array potential was monitored by a 100× high-voltage probe. The voltage probe, the current probes, and the high-voltage probe were connected to a four-channel digital oscilloscope, whose output was transferred to a lap-top computer. The oscilloscope was triggered when the array potential rose beyond -420 V.

The chamber is equipped with a planar langmuir probe of 6 mm diam that can be moved in the three axes. The probe is grounded through a 100-kΩ resistance. The current flowing into the probe is measured by reading the voltage across the 100-kΩ resistance by a voltage probe. The resistance of 100 kΩ was chosen so that the small amount of current, such as an ion saturation current in the density measurement, can be measured as the voltage across the resistance. At the same time, however, the cable connecting the probe has a capacitance of 600 pF to the ground, and currents with timescales faster than 100 kΩ $\times$ 600 pF $= 60$ μs cannot be measured directly. For such a fast varying current, only the time-integrated value can be measured as the voltage across the 600-pF capacitance that is parallel to the 100-kΩ resistance. The probe signal was also very susceptible to external high-frequency noise (2 MHz or higher). To minimize the effect of noise, we carried out the Fourier transform of all of the waveforms, including the currents and the voltage, and filtered out frequencies higher than 2 MHz. This filtering limited the time resolution of the experiment to 0.5 μs.

The current flowing to the probe consists of two parts. One part is the conduction current that is carried by charged particles entering the probe surface. The other part is displacement current that is due to the time variation of the surface charge induced on the probe surface as the electric field on the surface varies in time. Because the probe is fixed to the zero potential (chamber ground), there is always a potential difference from the surrounding plasma, and the probe is surrounded by a sheath. The probe surface and the sheath boundary forms a capacitance, and any change on the potential or the sheath thickness causes the change on the surface charge on the probe surface. When the potential near the probe changes rapidly, the probe surface charge also changes, and the displacement current flows between the probe and the ground. The displacement current basically corresponds to the time derivative of the electric potential near the probe.

In this paper, we mainly show the probe signal varying with the timescale of the orders of magnitude of 1 μs. Therefore, the probe signal should be regarded as the time-integrated value of the

probe current. Because the probe signal is the time integration of the probe current, the signal directly corresponds to the plasma potential around the probe. Then the probe acts as an ac potential probe (it cannot measure the dc potential) with the bandwidth between 16.6 kHz and 2 MHz. The positive probe signal means that the plasma potential around the probe is positive with respect to the probe. In that case, the probe signal mostly consists of the time-integrated displacement current because the conduction current due to ions is smaller in a short timescale of the order of magnitude of 1 μs. Therefore, the positive probe signal should be interpreted as an indicator of the plasma potential, though the probe signal voltage is not equal to the plasma potential. For the negative probe signal, the conduction current is as equally important as the displacement current. The interest is mostly in the positive probe signal.

The plasma uniformity inside the chamber was measured by the moving probe that measured the ion saturation current. When the temperature was assumed uniform, the plasma density decreased less than 10% between $y = 0$ and 70 cm as the position approached the chamber wall. In the z direction, the plasma density increased by a factor of two between $z = 10$ and 180 cm as the position approaches toward the plasma source. During the experiment, the plasma condition was monitored by a spherical (1-cm diam) langmuir probe that was fixed at $x = -30$ cm, $y = -80$ cm, and $z = 163$ cm.

In a typical case of the experiment, the bias voltage was set to a fixed value for 15 ~ 90 min, and we waited for arcs to occur. Arcs occur with a time interval of typically 10 ~ 30 s. This time is long enough for ions to recharge the insulator surface, producing the potential difference of several hundred volts. After a sufficient number of arcs, usually 5 ~ 20, occur, the moving probe is moved to a different position. The averages of currents and probe signals are taken from the data taken in one run.

III. Experimental Result and Discussion

In Figs. 5 and 6 examples of the measured waveforms are shown. In these examples, array 1 and capacitance 2 are biased to -500 V, and the probe is located at $z = 10$ cm and $y = 0$. Once an arc occurs, positive current flows from the array toward the ground, which we call discharge current. At the same time, negative current flows

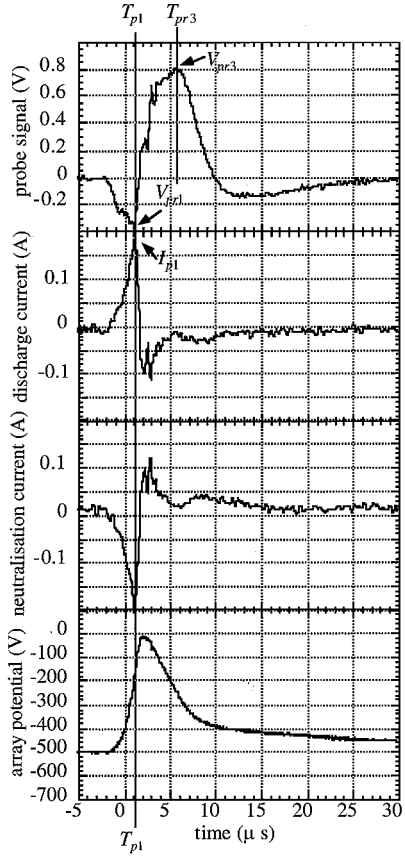

Fig. 5 Example of typical waveforms of 1-peak-type discharge.

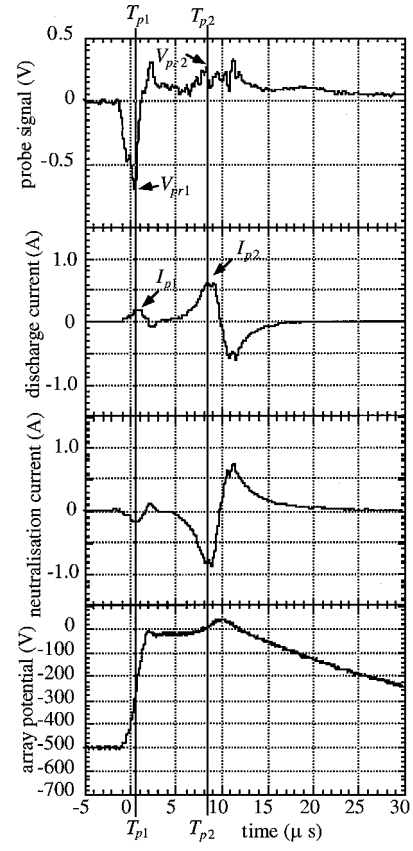

Fig. 6 Example of typical waveforms of 2-peak-type discharge.

from the capacitance, which we call neutralization current. The potential jumps to near zero value as a part of discharge current flowing through 10-kΩ resistance causes the voltage drop across the resistance. Once the potential jumps to near zero, the dc power supply is effectively decoupled from the array and the capacitance. Then the discharge current is supplied by the neutralization current and other stray capacitances in the circuit.

The potentials of the insulator surface ϕ_s is given by

$$\phi_s = \phi_e + Q_s/C_s \tag{1}$$

assuming that the insulator surface potential is uniform. Before an arc, the insulator surface has almost zero potential to attain the current zero condition. Then there is a potential difference nearly equal to the bias voltage V_b across the insulator. The charge stored by the insulator at a time t is given by

$$Q_s(t) = C_s(-V_b) + \int_0^t I_n \, \mathrm{d}t \tag{2}$$

Substituting Eq. (2) into Q_s of Eq. (1), we obtain

$$\phi_s = \phi_e + (-V_b) + \frac{\int_0^t I_n \, \mathrm{d}t}{C_s} \tag{3}$$

as the insulator surface potential. When the electrode potential jumps to near zero and while the charge flown as the neutralization current is still small, the insulator surface potential is approximated by

$$\phi_s \simeq -V_b \tag{4}$$

Similar analysis of the surface potential is presented in Ref. 5, where an ion acoustic wave launched from the insulator surface is also observed. There is also a report[12] of the optical measurement of the insulator surface potential at the arc onset.

The discharge current waveforms are categorized into two types. One is the type where the discharge current has only one peak, I_{p1}, as shown in Fig. 5, which we call 1-peak type. When 1-peak-type

discharge occurs, the probe signal first shows a negative peak V_{pr1} when the discharge current peaks at time T_{p1} and later shows positive peaks V_{pr3} at time T_{pr3}. The other waveform is the type where the discharge current has two peaks, as shown in Fig. 6, which we call the 2-peak type. The first peak I_{p1} is similar to that of the 1-peak type. The second peak I_{p2} occurs $5 \sim 15$ μs later, and it is usually larger than the first peak I_{p1}. The probe signal for the 2-peak type also shows a negative peak V_{pr1}, at the first peak of the discharge current, which is similar to the 1-peak type. When the discharge current has the second peak, however, the probe signal differs, depending on its position.

In the present experiment, we observed more than 1000 arcs. To judge whether each arc was 1-peak or 2-peak, we created a computer program. In the program, each discharge current waveform was first smoothed by taking the time average with the window size of 40 neighboring points to reduce the block noise associated with A/D conversion at the digital oscilloscope. In the smoothed waveform, the local peaks of 0.05 A or higher were searched. The criteria, 0.05 A and 40 data points, were determined after trial and error of the analysis. If there was a peak in the smoothed waveform, the program went back to the original waveform before smoothing and looked for the local maximum among the 40 points, then recorded its value and time. The program successfully identified the first peak I_{p1} for all of the waveforms analyzed. If the arc was 2-peak type, however, the program, occasionally, about 5% of all of the 2-peak types, gave more than two second peaks I_{p2} if the waveform had a large fluctuation that was not removed even after the low-path filtering with the 2-MHz criterion. In that case, the judgment was performed manually and the waveform was looked at with the naked eye.

It was common to 1-peak and 2-peak types that the probe signal shows a negative peak V_{pr1} at the first peak of the discharge current I_{p1}. Figure 7 shows the correlation between the two peaks. In this case, the probe position is at $y = 0$ and $z = 80$ cm, and array 2 and capacitance 1 are biased to $-500 \sim -800$ V. The data at different bias voltages are combined in Fig. 7. The probe negative peak V_{pr1} is proportional to the discharge current peak I_{p1}. Also, the data for 1-peak lie on the same line as the data for 2-peak. As far as the first peak I_{pr1} and the accompanying probe signal V_{pr1} are concerned, we see no significant difference between 1-peak- and 2-peak-type discharges. Once an arc occurs, the electrons are produced as the result of localized gas discharge near the interconnectors of the array.[13] The ions produced by the discharge are collected by the array and measured as the discharge current. The electrons produced by the discharge either neutralize the charges in the coverglass or are ejected into space. By the time the discharge current has the first peak I_{p1}, a positive charge of more than 10^{-7} C is already flown to the ground. This means that the same amount of negative charge is ejected to the chamber. If all of the charges stay in the chamber at the same time, the number of electrons, approximately 10^{12}, is about 10% of all of the electrons inside the chamber before the arc. This increase of the negative charge significantly lowers the chamber plasma potential. The plasma around the array becomes electron rich, and the space potential becomes negative due to the space charge of electrons. While the electrons travel toward the chamber wall or the capacitance surface to close the current circuit, the probe collects the electron conduction current giving the observed negative peak V_{pr1}.

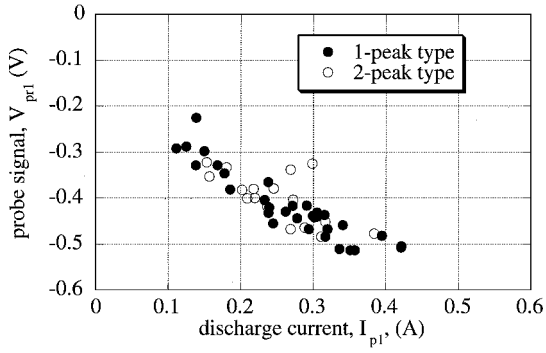

Fig. 7 Correlation between the first peak of discharge current I_{pr1} and probe signal V_{pr1}.

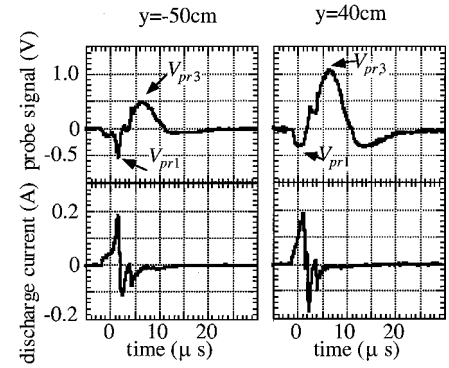

Fig. 8 Example of waveforms of probe signal and discharge current of 1-peak-type discharge measured at different positions along y axis.

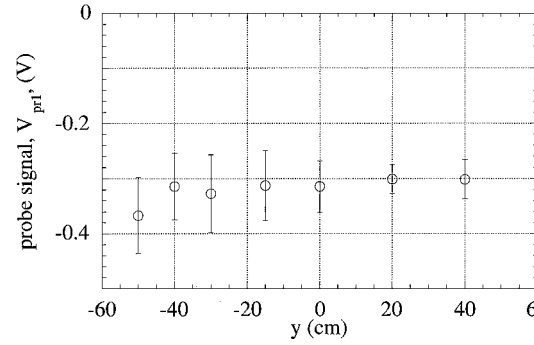

Fig. 9 Probe signal V_{pr1} at time of the first discharge current peak T_{p1} measured at different positions along y axis.

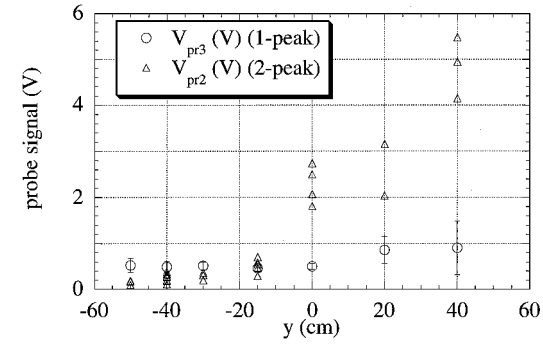

Fig. 10 Probe peak signal V_{pr3} for 1-peak-type discharge and probe signal V_{pr2} for 2-peak-type discharge measured at different positions along y axis.

Figure 8 shows examples of how the probe signal of 1-peak-type discharge changes depending on the probe y position. The second row of Fig. 8 shows the discharge current waveforms measured at the same time. In this case, array 2 located at $y = -70$ cm and capacitance 2 located at $y = 40$ cm are biased to -500 V, and the probe axial position is $z = 10$ cm. The discharge current has the first peak at $t = T_{p1} \simeq 1$ μs. The negative probe signal V_{pr1} at $t = T_{p1}$ (see Fig. 5 for definition) is observed even in front of the insulator ($y = 40$ cm), though it becomes smaller.

Figure 9 shows the probe signal V_{pr1} observed at different y positions, which are the results of the cases where array 2 ($y = -70$ cm) and capacitance 2 ($y = 40$ cm) were biased to -500 V. Figure 10 shows V_{pr3} and V_{pr2} for 2-peak-type discharge. In Fig. 9 the probe z axial position is $z = 10$ cm. To increase the number of sampling data, we combined data of the 1-peak- and 2-peak-type discharges, and each point is an average of at least eight measurements. Figure 9 shows that the probe signal V_{pr1} is more negative as the probe position approaches the array. In Ref. 11, it was shown that the probe signal V_{pr1} becomes more negative as the axial distance (z direction)

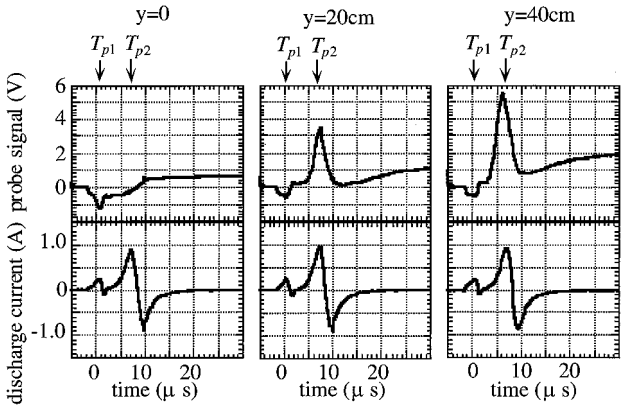

Fig. 11 Example of waveforms of probe signal and discharge current of 2-peak-type discharge measured at different positions along *y* axis.

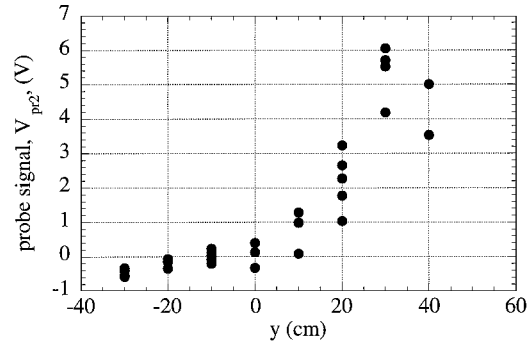

Fig. 12 Probe signal V_{pr2} at the second peak of 2-peak-type discharge measured at different positions along *y* axis.

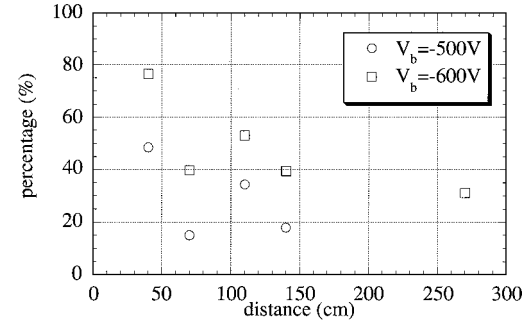

Fig. 13 Percentage of 2-peak-type discharge for different distances between array and capacitance.

from the array surface decreases. The results shown in Figs. 7–9 indicate that the electron-rich negative sheath is formed around the array within 2 or 3 μs from the arc onset regardless of the arc being 1-peak or 2-peak.

In Fig. 10, the positive peak value V_{pr3} (see Fig. 5) is shown for different y positions, which are the result of the cases where array 2 ($y = -70$ cm) and capacitance 2 ($y = 40$ cm) were biased to -500 V. The probe z axial position is $z = 10$ cm. In Fig. 10, we also plot the probe signal V_{pr2}, which will be explained later. For V_{pr3}, each point is an average of at least five measurements. Even if the current path is not formed between the array and the capacitance, the insulator surface potential jumps to a highly positive value as the electrode potential jumps. For the case shown in Fig. 10, array 2 and capacitance 2 were biased. At the arc onset the potential of the array and the capacitance electrode jumped from -500 V to near 0 V within 3 μs. The potential jump produces the positive sheath around the insulator surface. In Fig. 10, the position of $y = 40$ cm corresponds to the position in front of capacitance 2. Therefore, the positive sheath is centered at the insulator surface. The array position is $y = -70$ cm.

Figure 11 shows how the probe signal of 2-peak-type discharge changes depending on y position. The second row shows the discharge current waveforms measured at the same time. In this case, the array 1 located at $y = 0$ and the capacitance 2 located at $y = 40$ cm are biased to -600 V, and the probe axial position is $z = 10$ cm. The discharge current has the first peak at $t = T_{p1} \simeq 0.5$ μs and has the second peak at $t = T_{p2} \simeq 7$ μs for all three examples. When the probe is in front of the array ($y = 0$), the probe signal V_{pr2} at $t = T_{p2}$ (see Fig. 5 for notation) is negative, indicating that the influence of negative sheath formed at T_{p1} still remains even at time T_{p2}. When the probe approaches capacitance 2 ($y = 40$ cm), however, the probe signal V_{pr2} becomes more positive suggesting the presence of ion-rich positive sheath. Once an arc occurs, the potential of the solar array increases rapidly from the negative bias voltage to near zero, as shown in Fig. 6. The potential of the capacitance surface also increases suddenly from the near zero value to a positive value comparable to $|V_b|$, where $|V_b|$ is the bias voltage, as the potential of underlying electrode increases. Although the electrode and insulator surface potential increases within 3 or 4 μs from the arc onset, there is a time lag for the positive sheath to develop. It takes only 2 or 3 μs from the arc onset for the negative sheath to appear in front of the insulator surface. This time is even faster than the complete jump of the electrode potential. The positive sheath appears at $t \simeq T_{p2}$, which is nearly 10 μs from the arc onset. The mechanism of the positive sheath formation is further discussed in the experiment and the computer simulation in the companion paper (Ref. 9).

Figure 12 shows the dependence of V_{pr2} on the probe position for the combination of array 1 and capacitance 2 at the bias voltage of -600 V. In Fig. 12, $y = 0$ corresponds to array 1 and $y = 40$ cm corresponds to capacitance 2. The probe z position is 10 cm for all of the data points. Whether the probe signal V_{pr2} is positive or negative at $t = T_{p2}$ depends on whether the influence of the positive sheath from the insulator ($y = 40$ cm) exceeds the influence of the negative sheath from the array ($y = 0$ cm) or not. As the probe is placed closer to array 1 or beyond ($y \leq 0$), the probe signal becomes more negative because the influence of the negative sheath becomes greater. On the other hand, as the probe is placed closer to capacitance 2 ($y = 40$ cm), the probe signal becomes more positive because the influence of the positive sheath becomes greater. Because the probe signal is an indicator of the plasma potential, Fig. 12 indicates that there is a gradient in the plasma potential, that is, an electric field, from capacitance 2 to array 1, as shown in Fig. 3. If the conductivity of the plasma between the two surfaces is high enough, the current path is formed along the electric field, and the positive charge on the insulator surface is carried to the array as the arc current. The 2-peak-type discharge is the result of the current path formation, which is a RC discharge between the insulator and the array, where C is the capacitance of insulator and R is the resistance of the current path. At the second peak, we have a current of approximately 1 A (see Fig. 6 for an example). When it is assumed that the potential difference of the order of magnitude of 100 V exists between the insulator surface and the arc spot, the resistance of the current path is inferred to be of the order of magnitude of 100 Ω.

We now go back to Fig. 10, which shows the comparison between the signal V_{pr3} for 1-peak-type discharge and the signal V_{pr2} for 2-peak-type discharge. For the case of 1-peak-type discharge, the probe signal V_{pr3} increases near the capacitance, similar to V_{pr2}. However, V_{pr3} does not decrease nor become negative as V_{pr2} does. The two signals, V_{pr3} and V_{pr2}, indicates the presence of positive sheath near the capacitance surface. For the case of 2-peak-type discharge, the value of V_{pr2} near the capacitance is larger, by a factor of 4 or 5, than the value of V_{pr3}. This suggests that, when the 2-peak-type discharge occurs, the scale of positive sheath is larger. Also, for the case of 1-peak-type discharge, the signal V_{pr3} does not decrease nor become negative near the array, indicating the disappearance of negative sheath near the array. Whether an arc leads to the current path formation and 2-peak-type discharge or not depends on many factors. In the following discussion, we first focus on the distance between the two points because knowing how far the effect of an arc extends is an important technological issue. Later we discuss on the dependence on the bias voltage.

Figure 13 shows the percentage of 2-peak-type discharge for different combinations of biased array and capacitance. The horizontal

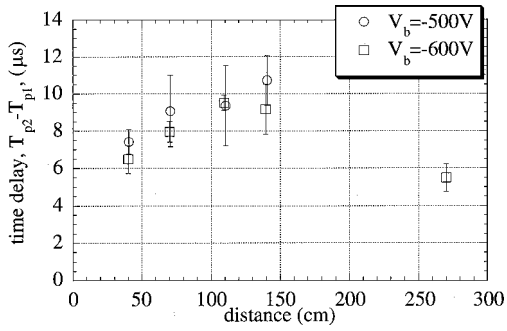

Fig. 14 Time delay between the first and second peaks in 2-peak-type discharge, $T_{p2} - T_{p1}$, for different distances between array and capacitance.

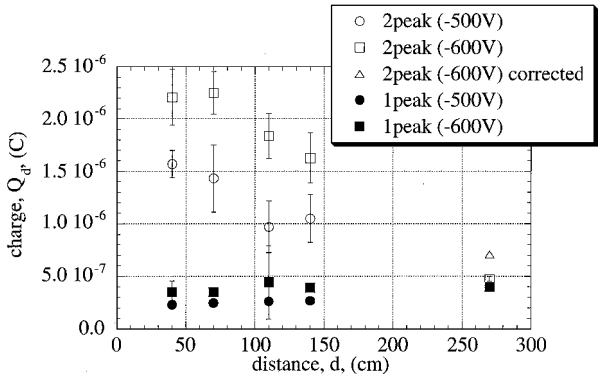

Fig. 15 Charge flown in one arc, Q_d, for different distances d between array and capacitance.

axis of Fig. 13 is given by the distance between the array and capacitance. The bias voltages are −600 and −500 V, and each data point is calculated from at least 32 arcs. Generally, the probability of occurrence of 2-peak type is less at longer distances because it is more likely that the negative sheath in front of the array and the positive sheath in front of the capacitance fail to meet as the distance becomes longer.

Figure 14 shows the time delay between the two peaks, $T_{p2} - T_{p1}$, for different combinations of biased array and capacitance. The horizontal axis of Fig. 14 is given by the distance between the array and capacitance. The bias voltages are −600 and −500 V, and each data point is calculated from at least nine arcs. The error bars in Fig. 14 indicate the standard deviation. Generally, the time delay is longer when the distance between the array and capacitance is longer because the longer the distance is, the longer time it takes for the positive and negative sheath to expand to form the current path. The exception is the case of 270 cm at −600 V, which corresponds to the bias combination of array 1 and capacitance 3. Array 1 and capacitance 3 are facing each other along the chamber axis. Then the sheaths expanding in the direction perpendicular to the surface, that is, z direction defined in Fig. 4, meet each other. The other cases shown in Fig. 14 correspond to the cases when either capacitance 1 or 2 is biased with one of the solar arrays, where the sheaths meet by expanding in the direction parallel to the surface. The speed of expanding sheath is probably different in the two directions, which will be shown in Ref. 9 via computer simulation.

Figure 15 shows the charge flown in one arc, Q_d, for different combinations of biased array and capacitance. The horizontal axis of Fig. 15 is given by the distance between the array and capacitance. The bias voltages are −600 and −500 V, and each data point is calculated from at least nine arcs. The error bars in Fig. 15 indicate the standard deviation. When the 2-peak-type discharge occurs, the charge flown in one arc is much larger than the 1-peak-type discharge. Therefore, the 2-peak-type discharge has more significant impact on the spacecraft system. For the case of 1-peak-type discharge, the charge is almost the same at $3.5 \sim 4.0 \times 10^{-7}$ C for all of the five cases of −600-V bias. The experimental circuit has a stray capacitance of 2.4 nF, mainly due to the coaxial cables used to bias the samples, which stores 1.4×10^{-6} C before an arc for the bias voltage of −600 V. That the charge for the 1-peak-type discharge does not depend on the distance between the array and the capacitance suggests that the charge from the stray capacitance is probably supplied as the arc current for the 1-peak-type discharge. For the case of 2-peak-type discharge, the charge stored on the insulator surface is also added to the arc current.

Even if the 2-peak-type discharge occurs, its scale decreases as the distance between the arced point and the unarced insulator surface becomes longer. Even if the current path is formed between the arced point and the insulator surface and the charge on the insulator is supplied as the arc current, not all of the charge on the insulator is released in one arc. Capacitances 1 and 2 have 21 nF, and the charge on the insulator surface before arc onset is 1.3×10^{-5} C for the bias voltage of −600 V. Because capacitance 3 has 5.2 nF, it has 3.1×10^{-6} C. To take into account that the capacitance for the case of 270 cm is one-quarter of the other four cases, we multiply the difference from the value of 1-peak-type discharge (0.8×10^{-7} C) by four and plot the corrected value for the 270-cm case by a triangle in Fig. 15. Then the data points of 2-peak-type discharge follow a single line. The least-square fit to the five data points gives

$$Q_d = 2.60 \times 10^{-6} - 6.96 \times 10^{-9} d \tag{5}$$

when the line is extended farther, how far the effect of one arc reaches on the charge of unarced insulator can be estimated. From Eq. (5), the distance of 374 cm is obtained as the point where the line crosses zero, and that is the longest distance one arc can extend its effect. The similar fit to the four data points for −500 V bias gives the distance of 297 cm as the safety distance.

We biased array 2 and capacitance 1 (separation distance 140 cm) at voltages between −500 and −800 V. The intention was to see the effect of bias voltage on the probability of occurrence of 2-peak-type discharge. At the beginning it was thought that the higher the bias voltage was, the more 2-peak-type discharges would be observed. However, as shown in Fig. 16, we saw no conclusive evidence of the dependence of the probability on the bias voltage. The percentage of 2-peak-type discharge increased as the bias voltage was raised from −500 to −600 V. This tendency was observed for all of the other separation distances, as shown in Fig. 13. However, from −600 to −800 V, the percentage did not change, showing little dependence on the bias voltage. The data of −500 and −600 V in Fig. 16 were calculated from 163 and 246 arcs, respectively. On the other hand, the data of −700 and −800 V were calculated from 58 and 55 arcs, respectively. To investigate whether or not the bias voltage affects the occurrence of 2-peak-type discharge, we probably need more experimental data.

Although we saw no clear evidence of the dependence of the probability of occurrence on the bias voltage, the time delay, $T_{p2} - T_{p1}$, had clear dependence on the bias voltage. Figure 17 plots the time delay between the two peaks, $T_{p2} - T_{p1}$, against the bias voltages. The bias combination is the same as Fig. 16, that is, array 2 and capacitance 1. In Fig. 17, each data point represents an average calculated from at least 21 measurements of the current waveforms, and the error bars indicate the standard deviation. Note that the higher

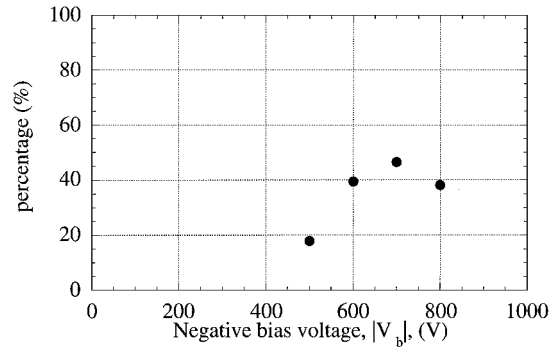

Fig. 16 Percentage of 2-peak-type discharge for different bias voltages applied to array 2 and capacitance 1.

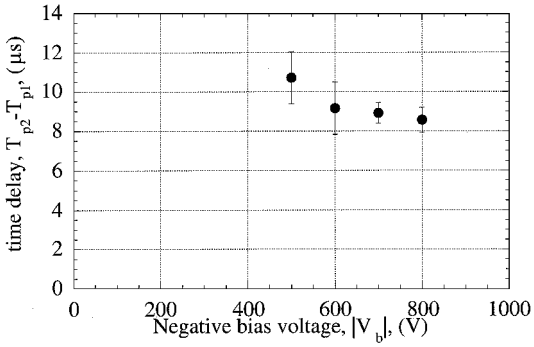

Fig. 17 Time delay between the first and second peaks in 2-peak-type discharge, $T_{p2} - T_{p1}$, for different bias voltages applied to array 2 and capacitance 1.

the bias voltage is, the shorter time it takes for the positive and negative sheath to expand to form the current path. Similar data from the previous experiment are also shown in Ref. 11.

IV. Conclusions

As the size of spacecraft systems and the demand for more power increases, arcing on solar array will become an obstacle against the development of megawatt-class space platforms that generate and deliver power at voltages of 400 V or higher. How an arc on solar array occurs has been well studied in previous work, and it has been known that the field intensification near the triple junction due to charging of insulator by plasma triggers the arc. To develop mitigation strategies against arcing on high-voltage space systems, both preventing arc onset and preventing its growth have practical importance. Laboratory experiments have been carried out to study how an arc on a solar array in the LEO plasma environment grows by taking charge from a remotely located insulator surface.

Once an arc occurs on a solar array, electrons are ejected from the arc spot. Initially the charge is supplied by the stray capacitance of the external circuit, such as the cable. Electrons diffuse away rapidly, and on their way, they produce a negative sheath around the arc point due to their negative space charge. At the same time, the jump in the circuit potential makes the insulator surface potential jump from near zero to a highly positive value. As the positive sheath reaches the arc point, there is an electric field between the array and the insulator. If the conductivity of the plasma along the field line is high enough, a current path is formed between the two points and carries the insulator charge and supplies the arc current, feeding energy to the arc plasma.

The experiment has shown that not all of the arc leads to the current path formation. If not, an arc is a just small pulse of current, that is, 1-peak-type discharge, whose scale is determined only by the stray capacitance connected to the circuit. If the current path is formed, that is, 2-peak-type discharge, it has a possibility of leading to a large-scale arc, even short circuiting of positive and negative ends of the solar array. The experimental results indicate that whether the current path is formed and how much the charge is released depends on how far the arc point and the insulator are separated. By extrapolating the experimental result, the safety distance of 3 ~ 4 m has been derived for bias voltages of −500 ~ −600 V. Of course, this number depends on the experimental condition, such as plasma density, neutral density, and others, and must be verified in a future experiment with a larger scale, possibly in a space experiment.

Acknowledgments

The authors thank K. Aihara of the Institute of Space and Astronautical Sciences and T. Matsumoto and K. Shiraishi, students of Kyushu Institute of Technology, for their help with the experiment.

References

[1]Sasaki, S., Naruo, Y., and Nagatomo, M., "Engineering Research for Solar Power Satellite SPS2000," *Proceedings SPS '97 Conference*, Montreal, PQ, Canada, 1997, pp. 73–77.

[2]Hastings, D. E., Cho, M., and Kuninaka, H., "The Arcing Rate for a High Voltage Solar Array: Theory, Experiment, and Predictions," *Journal of Spacecraft and Rockets*, Vol. 29, No. 4, 1992, pp. 538–554.

[3]Katz, I., Davis, V. A., and Snyder, D. B., "Mechanism for Spacecraft Charging Initiated Destruction of Solar Arrays in GEO," AIAA Paper 98-1002, Jan. 1998.

[4]Ferguson, D. C., Snyder, D. B., Vayner, B. V., and Galofaro, J. T., "Array Arcing in Orbit: from LEO to GEO," AIAA Paper 99-0218, Jan. 1999.

[5]Cho, M., Miyata, N., Hikita, M., and Sasaki, S., "Discharge over Spacecraft Insulator Surface in Low Earth Orbit Plasma Environment," *IEEE Transactions on Dielectrics and Electrical Insulation*, Vol. 6, No. 4, 1999, pp. 501–506.

[6]Vayner, B. V., Doreswamy, C. V., Ferguson, D. C., Galofaro, J. T., and Snyder, D. B., "Arcing on Aluminum Anodized Plates Immersed in Low-Density Plasma," *Journal of Spacecraft and Rockets*, Vol. 35, No. 6, 1998, pp. 805–811.

[7]Carruth, M. R., Jr., Vaughn, J. A., Bechtel, R. T., and Gray, P. A., "Experimental Studies on Spacecraft Arcing," *Journal of Spacecraft and Rockets*, Vol. 30, No. 3, 1993, pp. 323–327.

[8]Vaughn, J. A., Carruth, M. R., Jr., Katz, I., Mandell, M. J., and Jongeward, G. A., "Electrical Breakdown Currents on Large Spacecraft in Low Earth Orbit," *Journal of Spacecraft and Rockets*, Vol. 31, No. 1, 1994, pp. 54–59.

[9]Cho, M., Ramasamy, R., Hikita, M., Tanaka, K., and Sasaki, K., "Plasma Response to Jump of Insulator Surface Potential in Ionospheric Plasma Environment," *Journal of Spacecraft and Rockets*, Vol. 39, No. 3, 2002, pp. 400–408.

[10]Carruth, M. R., Jr., Schneider, T., McCollum, M., Ferguson, D., Katz, I., Mickaterian, R., Alred, J., and Pankop, C., "ISS and Spaced Environment Interactions Without Operating Plasma Contactor," AIAA Paper 2001-0401, Jan. 2001.

[11]Cho, M., Hikita, M., Tanaka, K., and Sasaki, S., "Transient Phenomena Induced by Discharge on Solar Array in Low Earth Orbit Plasma Environment," *IEEE Transactions on Plasma Science* (to be published).

[12]Cho, M., Miyata, N., and Hikita, M., "Effects of Arcing on Insulator Surface Charging Condition in Plasma Environment," AIAA Paper 2000-0872, Jan. 2000.

[13]Cho, M., and Hastings, D. E., "Computer Particle Simulation of High Voltage Solar Array Arcing Onset," *Journal of Spacecraft and Rockets*, Vol. 30, No. 2, 1992, pp. 189–201.

A. C. Tribble
Associate Editor